

Characterization of p-GaN_{1-x}As_x/n-GaN PN Junction Diodes

H. Qian,^{1,a)} K. B. Lee,¹ S. Hosseini Vajargah,² S. V. Novikov,³ I. Guiney,² S. Zhang,² Z. H. Zaidi,¹ S. Jiang,¹ D. J. Wallis,² C. T. Foxon,³ C. J. Humphreys,² and P. A. Houston¹

¹*Department of Electronic and Electrical Engineering, University of Sheffield, Sheffield S1 3JD, UK*

²*Department of Material Science and Metallurgy, University of Cambridge, Cambridge CB3 0FS, UK*

³*School of Physics and Astronomy, University of Nottingham, Nottingham NG7 2RD, UK*

The structural properties and electrical conduction mechanisms of p-type amorphous GaN_{1-x}As_x/n-type crystalline GaN PN junction diodes are presented. A hole concentration of $8.5 \times 10^{19} \text{ cm}^{-3}$ is achieved which allows a specific contact resistance of $1.3 \times 10^{-4} \Omega\text{-cm}^2$. An increased gallium beam equivalent pressure during growth produces reduced resistivity but can result in the formation of a polycrystalline structure. The conduction mechanism is found to be influenced by the crystallinity of the structure. Temperature dependent current voltage characteristics at low forward bias ($<0.35 \text{ V}$) show that conduction is recombination dominated in the amorphous structure whereas a transition from tunneling to recombination is observed in the polycrystalline structure. At higher bias, the currents are space charge limited due to the low carrier density in the n-type region. In reverse bias, tunneling current dominates at low bias ($<0.3 \text{ V}$) and recombination current becomes dominant at higher reverse bias.

1. Introduction

GaN-based PN diodes are attractive for power electronic applications due to the high breakdown field and low power loss and are likely to play an important part in supporting the required large voltages in vertical power devices. However, achieving a high hole concentration ($>10^{18} \text{ cm}^{-3}$) remains difficult due to the high activation energy of Mg dopants which can result in high resistivity and poor ohmic contacts. Mg-doped p-type amorphous GaN_{1-x}As_x ($0.17 < x < 0.8$) with band gaps varying from 0.8-3.4 eV have been demonstrated previously with high hole concentrations up to $1 \times 10^{20} \text{ cm}^{-3}$ [1,2]. The high hole concentration can be used to improve the performance of electronic devices such as PN diodes, p-GaN gated HFETs and JFETs. However, reports on the characteristics of the material in electronic devices is still lacking. In this paper, for the first time, we present a study of the electrical characteristics of p-GaN_{1-x}As_x/n-GaN junction diodes and include the structural properties and transport mechanisms.

^{a)} Electronic mail: hqian2@sheffield.ac.uk.

2. Device fabrication

The diode structure is shown in Fig. 1. Firstly, n-GaN templates with a 500 nm n+GaN contact layer with a Si concentration of $\sim 5 \times 10^{18} \text{ cm}^{-3}$ and 2.5 μm GaN drift layer with Si concentration of $\sim 2 \times 10^{16} \text{ cm}^{-3}$ were grown using metal-organic chemical vapour deposition (MOCVD) on sapphire substrates. Subsequently, the sample was transferred (in air ambient) into a plasma assisted molecular beam epitaxy (MBE) chamber for 1 μm GaN_{1-x}As_x regrowth. Two samples (sample 1 and 2) were grown at different Ga beam equivalent pressures (BEPs) of 2.3×10^{-7} and 2.1×10^{-7} Torr, respectively. These Ga BEPs were chosen to enable growth with the lowest resistivity which, as will be discussed later, is also close to the conditions where a transition between amorphous and polycrystalline is possible. The As₂ and Mg BEPs were kept at 6.6×10^{-6} and 6×10^{-9} Torr and the substrate temperature was held at 245 °C during growth for both samples. The detailed growth mechanisms can be found elsewhere [1,2]. In addition, a set of GaN_{1-x}As_x calibration layers were grown to study the dependence of resistivity and contact resistance on Ga BEP which was specified between 1.3×10^{-7} to 2.2×10^{-7} Torr.

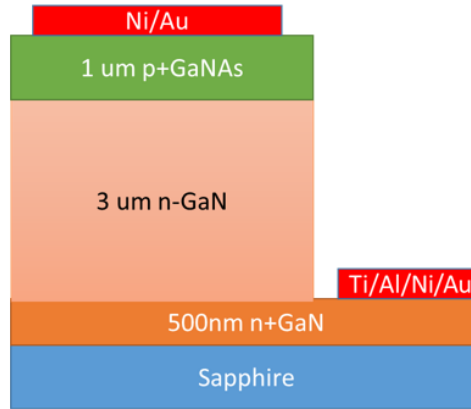


Fig. 1. Device structure of GaN/ GaN_{1-x}As_x PN junction diode.

The mesa diode was patterned by standard lithography with an active area of $1.2 \times 10^{-3} \text{ cm}^2$ and dry-etched in an inductively coupled plasma system with Cl₂-based gases to access the n+GaN current spreading layer. Ti/Al/Ni/Au and Ni/Au contacts were deposited using a thermal evaporator as the cathode and anode, respectively. It is worth mentioning that most Ni-based ohmic contacts formed on p-GaN in the literature required a post-deposition annealing in O₂ ambient to achieve a good ohmic contact [3,4]. However, in our samples, post-deposition annealing was not required due to the high carrier concentration in the p-type material.

3. Results and discussion

3.1 Properties of GaN_{1-x}As_x layer

Room temperature Hall-effect measurements were carried out with a GaN_{1-x}As_x calibration sample grown on sapphire with a Ga BEP of 2.3×10^{-7} Torr. A hole concentration of $8.5 \times 10^{19} \text{ cm}^{-3}$ and a mobility of $0.15 \text{ cm}^2 \text{ V}^{-1} \text{ s}^{-1}$ were extracted. Circular transmission line model (CTLM) structures were used to study the dependence of specific contact resistance (ρ_c) and resistivity on the Ga BEP. As shown in fig. 2, a clear reduction of ρ_c and resistivity are observed with increased Ga BEP. With Ga BEP increased to 2.2×10^{-7} Torr, ρ_c and the resistivity reduced to $1.3 \times 10^{-4} \text{ } \Omega\text{-cm}^2$ and $0.5 \text{ } \Omega\text{-cm}$, respectively, which are lower than those typically achieved in conventional p-GaN [5-8]. However, it is known that an increased Ga BEP can result in the formation of polycrystalline clusters embedded in the amorphous matrix [2]. Our approach was to grow the highest possible conductivity layers while avoiding the formation of polycrystalline structures.

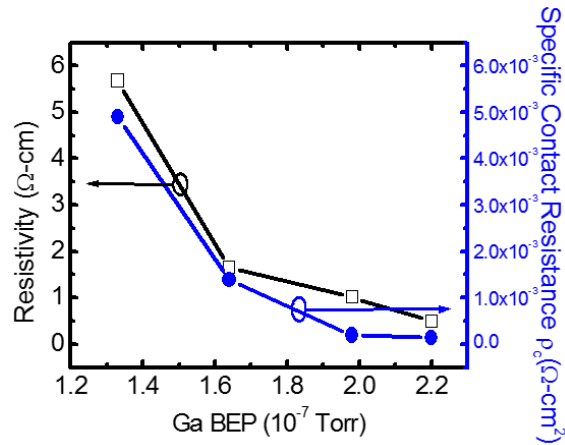


Fig. 2. Dependence of GaNAs resistivity (black) and specific contact resistance (blue) on Ga flux during growth.

Fig. 3(a) shows the transmission electron microscopy (TEM) images of the PN diode samples. An all-polycrystalline structure was observed in sample 1 (Ga BEP 2.3×10^{-7} Torr). When the Ga BEP was reduced to 2.1×10^{-7} Torr in sample 2, as shown in Fig. 3(b), the growth started with an amorphous layer ($\sim 350 \text{ nm}$) followed by a polycrystalline layer which can be identified by the electron diffraction patterns. It is thought that the transition occurred as a result of Ga accumulation with a resultant effective increase in BEP during growth.

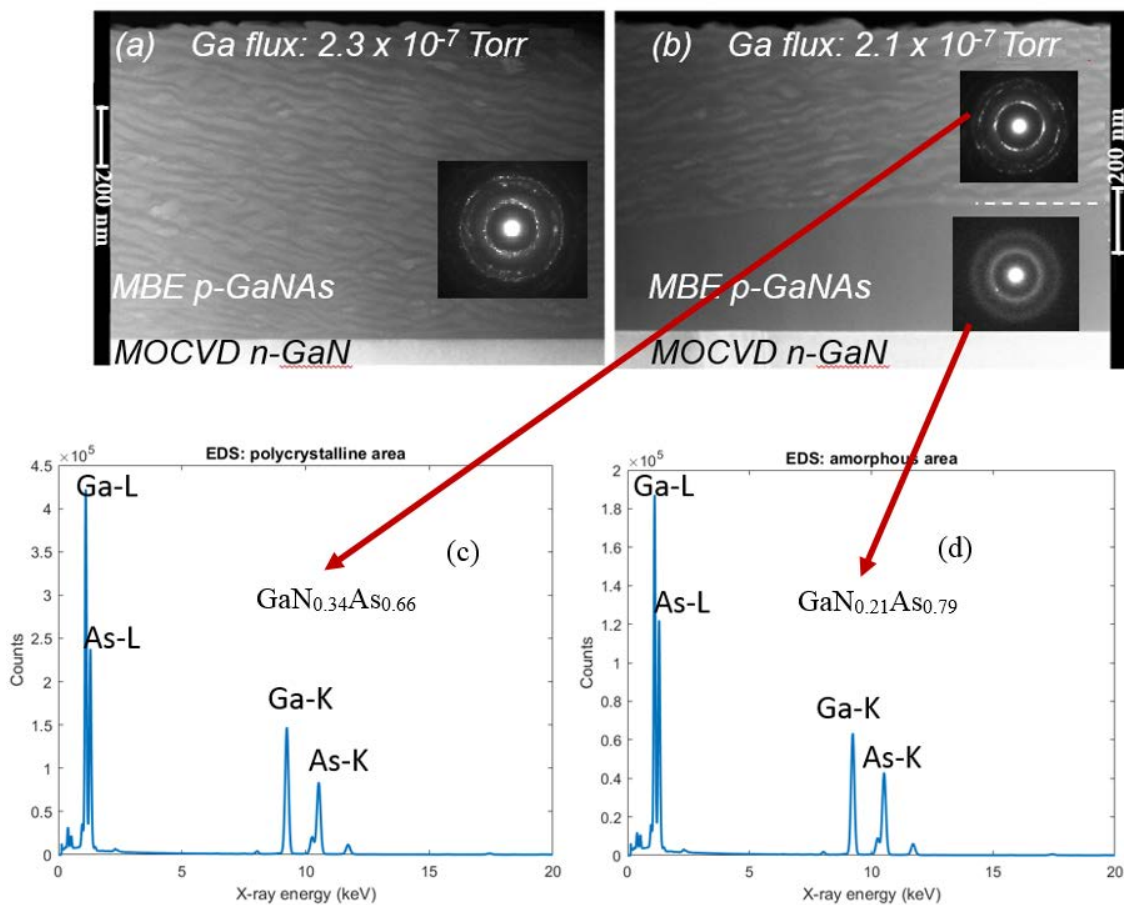


Fig. 3. TEM images with electron diffraction patterns of GaNAs layers showing (a) sample 1 (all-polycrystalline structure), and (b) sample 2 (amorphous/polycrystalline structure); EDS results showing the composition of (c) polycrystalline region, and (d) amorphous region.

We were unable to detect any PL or CL signal from amorphous $\text{GaN}_{1-x}\text{As}_x$ layers, similar to what was observed in our previous studies [1,2]. Energy dispersive x-ray spectroscopy (EDS) analysis was carried out on sample 2 to determine the average composition of each region. As shown in Fig. 3 (c) and 3 (d), $\text{GaN}_{0.34}\text{As}_{0.66}$ and $\text{GaN}_{0.21}\text{As}_{0.79}$ compositions were measured in the polycrystalline and amorphous regions, respectively. The corresponding band gap energies (~ 1 eV) are estimated according to the band anti-crossing model and previously published results [1].

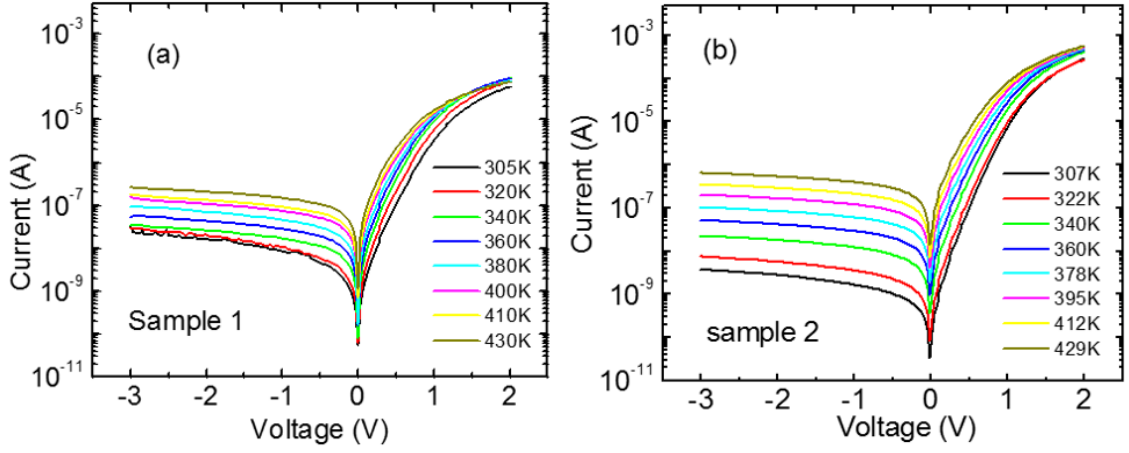


Fig.4. Temperature dependent IV characteristics on semi-log scale of (a) sample 1, and (b) sample 2.

3.2 Current conduction mechanisms in the PN junctions

The room temperature turn-on voltages (defined at 10 mA/cm²) for sample 1 and 2 are 1.29 and 1.07 V, respectively. Fig. 4(a) and 4(b) show the temperature dependent current-voltage (I - V - T) characteristics for sample 1 and 2 measured over the temperature range of 305 – 430 K on a semi-log scale. The forward currents increase exponentially at low bias (<0.35 V) and non-exponentially at higher bias voltage. In order to identify the dominant current conduction mechanism at low bias regime, the reverse saturation current I_0 and ideality factor n is extracted by fitting to the Shockley model described by [9]:

$$I = I_0 \left[\exp \left[\frac{q(V - IR_s)}{nkT} \right] - 1 \right] \quad (1)$$

where R_s is the series resistance, k the Boltzmann constant and T the temperature. In the classical generation-recombination (G-R) model, n lies between 1-2 and is independent of temperature and I_0 is characterized by:

$$I_0 \propto \exp \left[-\frac{E_{ac}}{2kT} \right] \quad (2)$$

where E_{ac} is the activation energy that describes the energy of the recombination site. Good curve fitting was obtained at the low bias regime (< 0.35V) where series resistance and high injection effect are insignificant. The room temperature ideality factors extracted from sample 1 and sample 2 are 4.3 and 3.5, respectively. Several groups have reported ideality factors greater than two in GaN PN junctions which contradicts the G-R model. The exact reason for the high ideality factor in our samples is unclear. Shah et al. [10] attributed this behavior to the summation of n of each rectifying junction within the structure, including the contacts. In our case, although the contacts are ohmic as confirmed by CTLM measurements, at low currents the n+/n-GaN junction might contribute to additional n due to the abrupt change in doping profile. Another

possibility, as explained by Hurni et al. [8], is due to the high density of interfacial defects, dislocations and non-uniformity of the doping.

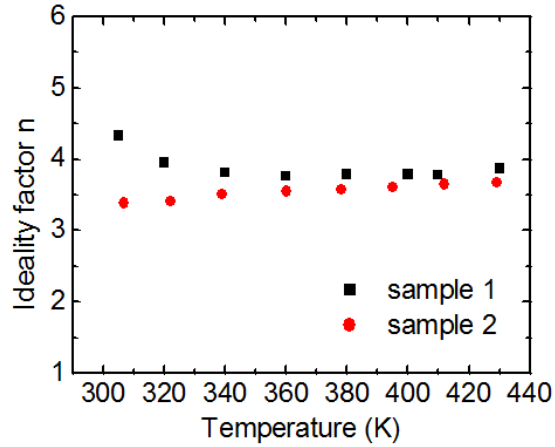


Fig.5. Temperature dependent of ideality factor n

On the other hand, a tunneling current in the junction may also result in $n > 2$ which can be identified when n is inversely proportional to T [11-14]. The plot of n versus T is given in Fig. 5. In sample 1, n reduces to 3.8 when T increases to 340 K which is a signature of a tunneling mechanism. Within this temperature range, $\ln(I_0)$ is observed to be proportional to T which can be described by a multi-step tunneling mechanism similar to amorphous silicon PN junctions [12] and GaN LEDs [15]. As a polycrystalline structure, tunneling is expected at the grain boundaries between the crystallites [16]. In addition, the high density of defects within the crystallites may also act as mid-gap states and lead to defect-assisted tunneling. Above 340 K, n becomes independent of T indicating a possible transition to the G-R mechanism. A similar transition process was also observed in wafer fused GaN/GaAs diodes [17].

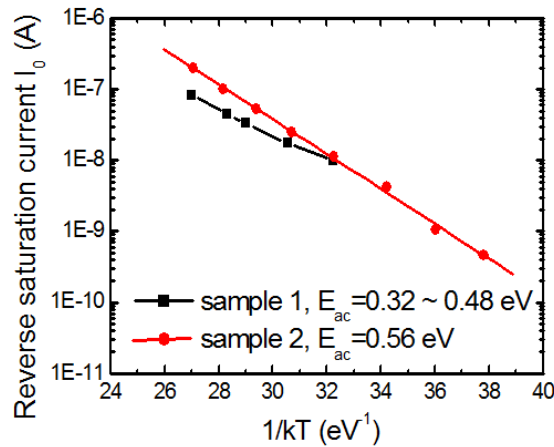


Fig.6. Arrhenius plot of I_0 . Sample 1 is tunneling dominated at temperatures below 340 K therefore not shown in the Arrhenius plot.

Fig. 6 shows the Arrhenius plot of I_0 to determine the energies of the recombination sites. However, a non-linear fit was observed for sample 1 whereas one would expect a straight line in the case of recombination dominated conduction. A similar non-linearity has been observed in polysilicon PN diodes [16] where two activation energies were obtained, indicating the presence of two energy levels within the band gap. In our case, the activation energy gradually increases from 0.32 to 0.48 eV as the temperature increases, which may indicate multiple energy levels distributed within the band gap. It is speculated that the recombination process occurs at the lower energy tunneling sites at low temperature and, as temperature increases, higher energy levels are involved which moves the activation energy towards higher values. In sample 2, on the other hand, n remains almost constant throughout the temperature range. $\ln(I_0)$ is observed to have a linear dependence on $1/kT$ which is consistent with eq. 2. $E_{ac} = 0.56$ eV is extracted from Arrhenius plot which is in agreement with the estimated half band gap value for $\text{GaN}_{0.21}\text{As}_{0.79}$. This is an indication that recombination in the amorphous $\text{GaN}_{0.21}\text{As}_{0.79}$ part of the depletion region dominates the conduction.

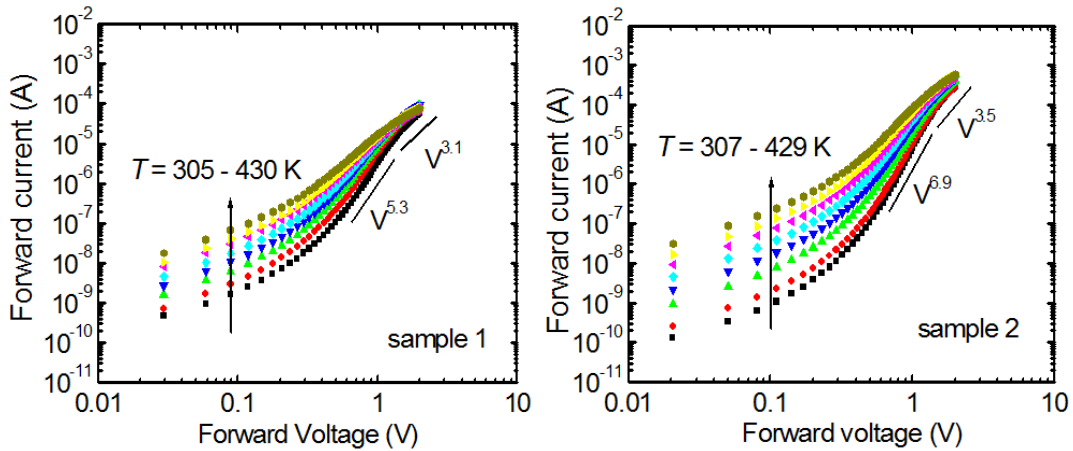


Fig.7. Forward current characteristics on a log-log scale of (a) sample 1, and (b) sample 2.

Fig. 7 shows the forward current characteristics on a log-log scale. At the higher bias (>0.35 V), the currents follow a power law (V^m) dependence in both samples. The value of m is greater than two which indicates that the current is space charge limited [14]. This is understandable as the electron concentration of the drift layer is more than three orders of magnitude lower than the hole concentration in the p-type region, and a space charge limited region forms at high current injection levels. The reduced m at higher bias indicates the conduction is moving towards a series resistance limited region.

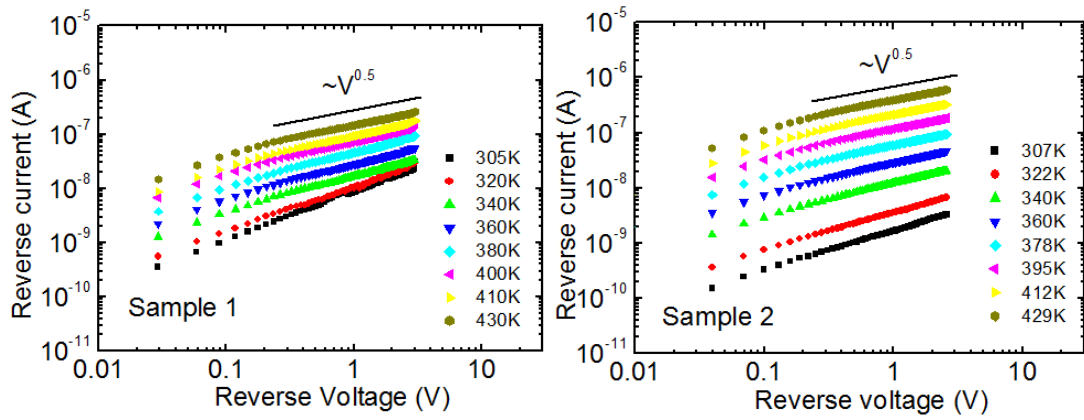


Fig.8. Reverse current characteristics on a log-log scale of (a) sample 1, and (b) sample 2.

Fig. 8 shows the temperature dependent reverse currents plotted against reverse voltage V_r on a log-log scale. Two distinctive regions can be seen in both samples. At $V_r > 0.3$ V (except $T < 340$ K regime in sample 1), the reverse currents follow a $V^{0.5}$ dependence which is known to be the generation current within the depletion region [14]. The Arrhenius plots of the reverse currents at 0.5 V yield activation energies of 0.28 to 0.37 eV for sample 1 and 0.52 eV for sample 2. The increase of activation energy of sample 1 is believed to be due to a similar behavior as in the low forward bias regime which involves multiple energy levels. At $V_r < 0.3$ V, the reverse currents do not follow the $V^{0.5}$ relationship but are found to have a similar T dependence as in the multi-step tunneling case. Additionally, a similar trend is observed in sample 1 for all applied voltages at $T < 340$ K. This behavior coincides with the transition from tunneling to recombination under forward bias in sample 1.

4. Discussion

Several groups observed significantly reduced turn-on voltage in regrown GaN diode structures which were attributed to tunneling current through interfacial defect states [17-19]. In other words, the diode characteristics were dominated by the interfacial states instead of the band discontinuity and junction built-in potential. In order to evaluate the contribution of the interface states in our samples, one needs to first estimate the built-in potential (V_{bi}) which is approximately equal to the band gap of $\text{GaN}_{1-x}\text{As}_x$ (~ 1 eV) plus the conduction band offset [1]. However, the theoretical value of V_{bi} cannot be determined in this case as the conduction band offset ΔE_c and electron affinity of $\text{GaN}_{1-x}\text{As}_x$ are unknown. From the I - V measurement, the turn-on voltages (1.29 and 1.07 V) are close to the estimated band gap values of the respective $\text{GaN}_{1-x}\text{As}_x$. So the turn-on voltage in our case cannot be as heavily dominated by interfacial states as in [17]. However, the possibility of early turn-on cannot be ruled out since the theoretical value of V_{bi} is unknown, unless the ΔE_c is reduced to zero due to interface grading. In

fact, an early turn-on is very likely to happen as tunneling current is observed in the sample as revealed by the I - V - T experiment.

Caution must be observed in interpreting the “non-physical” ideality factor ($n > 2$) presented in both samples despite the fact that they show G-R dominated characteristics. This may be due to the existence of tunneling caused by the defects within the structure. In our samples, the dangling bond at the GaN surface and the impurities incorporated during the transfer before MBE regrowth can contribute mid-gap states presents at the GaN/GaN_{1-x}As_x interface. In addition, defects within the bulk semiconductors can also contribute to tunneling current.

5. Conclusion

We have studied the structural and electrical characteristics of GaN_{1-x}As_x/GaN PN diodes. The material transits from amorphous into polycrystalline with increased Ga BEP. The formation of an amorphous layer with low resistivity requires careful control of the Ga BEP during growth. The transport mechanism is greatly influenced by both interfacial and bulk defects. At low forward bias, G-R process is the possible dominating mechanism in the amorphous structure whereas a possible transition from tunneling to recombination is observed in the polycrystalline structure. At high forward bias, the currents show space charge limited characteristics due the low carrier density in the n-type region. In reverse bias, tunneling current dominates at low voltage and becomes recombination dominated at higher bias. The high hole concentration is beneficial for good ohmic contacts and shows promise for low-loss GaN-based power diodes and JFETs. Practical diodes designed to withstand high reverse breakdown voltage will likely require less As concentration in order to increase the band gap so that the carrier generation and tunneling are limited.

Acknowledgement

This work was undertaken with support from the EPSRC (EP/K014471/1). The authors would like to acknowledge Prof. K.M. Yu and Prof. W. Walukiewicz for discussions.

References

[1] S. V. Novikov, C. R. Staddon, C. T. Foxon, K. M. Yu, R. Broesler, M. Hawkridge, Z. Liliental-Weber, J. Denlinger, I. Demchenko, F. Luckert, P. R. Edwards, R. W. Martin, W. Walukiewicz, “Growth by molecular beam epitaxy of amorphous and crystalline GaNAs alloys with band gaps from 3.4 to 0.8 eV for solar energy conversion devices”, *Journal of Crystal Growth* 323 (2011) 60–63

- [2] A. X. Levander, S. V. Novikov, Z. Liliental-Weber, R. dos Reis, O. D. Dubon, J. Wu, C. T. Foxon, K. M. Yu, and W. Walukiewicz, "Doping of GaN_{1-x}As_x with high As content", *Journal of Applied Physics* 110, 093702 (2011)
- [3] J. -K. Ho, C. -S. Jong, C. -C. Chiu, C. -N. Huang, K. -K. Shih, L. -C. Chen, F. -R. Chen, and J. -J. Kai, "Low-resistance ohmic contacts to p-type GaN achieved by the oxidation of Ni/Au films", *Journal of Applied Physics* 86, 4491 (1999)
- [4] X. J. Li, D. G. Zhao, D. S. Jiang, Z. S. Liu, P. Chen, J. J. Zhu, L. C. Le, J. Yang, X. G. He, S. M. Zhang, B. S. Zhang, J. P. Liu, and H. Yang, "The significant effect of the thickness of Ni film on the performance of the Ni/Au Ohmic contact to p-GaN", *Journal of Applied Physics* 116, 163708 (2014)
- [5] J. -D. Hwang, Z. -Y. Lai, C. -Y. Wu and S. -J. Chang, "Enhancing p-type conductivity in Mg-doped GaN using oxygen and nitrogen plasma activation", *Japanese Journal of Applied Physics*, Vol. 44, No. 4A, (2005), pp. 1726–1729
- [6] M. Scherer, V. Schwegler, M. Seyboth, C. Kirchner, M. Kamp, A. Pelzmann, and M. Drechsler, "Low resistive p-type GaN using two-step rapid thermal annealing processes", *Journal of Applied Physics* 89, 8339 (2001)
- [7] A. Dussaigne, B. Damilano, J. Brault, J. Massies, E. Feltin, and N. Grandjean, "High doping level in Mg-doped GaN layers grown at low temperature", *Journal of Applied Physics* 103, 013110 (2008)
- [8] C. A. Hurni, J. R. Lang, P. G. Burke, and J. S. Speck, "Effects of growth temperature on Mg-doped GaN grown by ammonia molecular beam epitaxy", *Applied Physics Letters* 101, 102106 (2012)
- [9] C. T. Sah, R. N. Noyce, and W. Shockley, "Carrier generation and recombination in P-N junctions and P-N junction characteristics", *Proc. IRE* 45, 1228 (1957)
- [10] J. M. Shah, Y. -L. Li, Th. Gessmann, and E. F. Schubert, "Experimental analysis and theoretical model for anomalously high ideality factors ($n \gg 2.0$) in AlGaIn/GaN p-n junction diodes", *Journal of Applied Physics* Vol. 94, No. 4, (2003)
- [11] J. B. Fedison, T. P. Chow, H. Lu, and I. B. Bhat, "Electrical characteristics of magnesium-doped gallium nitride junction diodes", *Applied Physics Letters*, 72(22), 2841–2843 (1998)
- [12] A. J. Harris, R. S. Walker, and R. Sneddon, "Current-voltage characteristics of amorphous silicon PN junctions", *Journal of Applied Physics* 51, 4287 (1980)
- [13] H. Matsuura, T. Okuno, H. Okushi, and K. Tanaka, "Electrical properties of n-amorphous/p-crystalline silicon heterojunctions", *Journal of Applied Physics* 55, 1012 (1984)
- [14] H. Mimura and Y. Hatanaka, "Carrier transport mechanisms of p-type amorphous-n-type crystalline silicon heterojunctions", *Journal of Applied Physics* 71, 2315 (1992)
- [15] Q. Shan, D. S. Meyaard, Q. Dai, J. Cho, E. F. Schubert, J. K. Son, and C. Sone, "Transport-mechanism analysis of the reverse leakage current in GaInN light-emitting diodes", *Applied Physics Letters* 99, 253506 (2011)
- [16] M. Dutoit and F. Sollberger, *J. Electrochem*, "Lateral Polysilicon p-n Diodes", *Solid-state Science and Technology*, Vol. 125, No. 10, 1648 (1978)
- [17] Chuanxin Lian, Huili Grace Xing, Yu-Chia Chang and Nick Fichtenbaum, "Electrical transport properties of wafer-fused p-GaAs/n-GaN Heterojunctions", *Applied Physics Letters* 93, 112103 (2008)

[18] Erik Danielsson, Carl-Mikael Zetterling, Mikael Östling, Andrey Nikolaev, Irina P. Nikitina and Vladimir Dmitriev, "Fabrication and Characterization of Heterojunction Diodes with HVPE-Grown GaN on 4H-SiC", IEEE Transactions On Electron Devices, Vol. 48, No. 3 (2001)

[19] John T. Torvik, Chang-hua Qiu, Moeljanto Leksono and Jacques I. Pankove, "Optical characterization of GaN/SiC n-p heterojunctions and p-SiC", Applied Physics Letters, Volume 72, Number 8 (1998)